

# Measurement of ferric ion diffusion coefficient in Fricke-infused agarose gel from MR image intensity changes

Yin-Jiun Tseng,<sup>1</sup> Woei-Chyn Chu,<sup>1,2</sup> Sung-Cheng Huang<sup>3</sup>

<sup>1</sup>Institutes of Biomedical Engineering and <sup>2</sup>Radiological Sciences

National Yang Ming University, Pei-Tou, Taipei, Taiwan, ROC

<sup>3</sup>Dept. of Molecular and Medical Pharmacology and Laboratory of Structural Biology and Molecular Medicine (DOE), UCLA School of Medicine, Los Angeles, California

**Abstract**-A mathematical modeling was adopted to calculate the ferric ion diffusion coefficient based on the radiation induced magnetic resonance (MR) image intensity change in Fricke-agarose gels. A fast magnetic resonance imaging acquisition technique was employed to avoid the smearing of acquired data due to diffusion over an extended period of time. Our results showed that for a Fricke-agarose gel contained 1mM ammonium ferrous sulfate, 1% agarose, 1mM sodium chloride and 50mM sulfuric acid, its ferric ion diffusion coefficient is  $1.31 \times 10^{-2} \text{cm}^2 \text{h}^{-1}$  in room temperature. This value falls within the  $1 \sim 2 \times 10^{-2} \text{cm}^2 \text{h}^{-1}$  range obtained by previous studies under varying concentrations of gel ingredients.

**Keywords**- MRI- Fricke-infused gel dosimetry, ferric ion diffusion, gamma knife radiosurgery

## I. INTRODUCTION

Due to its high sensitivity, superior tissue equivalence and three-dimensional characteristics, the Fricke-infused gels have been used in various radiation dosimetry applications [1]. However, its measurement accuracy has been seriously affected by the ferric ion diffusion contamination [2, 3]. It is therefore important to find out the magnitude of ferric ion diffusion coefficient under specific dosimetric experiment conditions [4, 5].

Based on a set of MR images acquired under different ferric ion diffusion effect, a least square post-processing method was used to calculate the ferric ion diffusion coefficient. The corresponding dose distribution profile evolutions can be recorded from these MR image intensity changes [6]. Because for each MR acquisition is several folds faster than the conventional R1-based dosimetry methods, it therefore suffers much less smearing of the dose profiles and enables a more efficient way to calculate ferric ion diffusion coefficient.

## II. METHODOLOGY

### 1) Diffusion:

Diffusion is governed by the following equation,

$$D \nabla^2 \rho = -\frac{\partial \rho}{\partial t}, \quad (1)$$

where  $D$  is the diffusion coefficient and  $\rho$  is the concentration distribution. Given an initial concentration distribution at  $t = 0$ ,  $\rho(x, y, z, 0)$ , the concentration distribution at  $t = T$ ,  $\rho(x, y, z, T)$  can be solved by

$$\tilde{\rho}(\mathbf{k}, t) = \tilde{\rho}(\mathbf{k}, 0) \exp(-D|\mathbf{k}|^2 t), \quad (2)$$

where  $\tilde{\rho}(\mathbf{k}, 0)$  is the Fourier Transform of  $\rho(x, y, z, 0)$ .

### 2) Point dose calculation algorithm:

In our simulation model, the initial concentration distribution at  $t = 0$ ,  $\rho(x, y, z, 0)$ , was regarded to be the initial dose distribution in a  $32 \times 32 \times 32$  pixels region centered at the gamma knife focal point where the dose of each point in the interest volume can be determined based on the inverse square law and the linear attenuation exponential formula.

### 3) Gamma Knife irradiation:

Irradiation of the Fricke-agarose gel phantom was performed using a Leksell gamma knife-B type. A maximum dose of 40 Gy was delivered to the center of the gel phantom using a 14 mm collimator.

### 4) Fricke-agarose gel preparation:

The Fricke-agarose gel was prepared by first mixing a desired amount of agarose powder with 1500 mL triple distilled water and was heated and maintained at the temperature ( $95^\circ\text{C}$ ) until agarose powder was completely dissolved. Then it was moved to a water bath for cooling until the temperature reached  $60^\circ\text{C}$ . A ferrous sulfate solution consisting of a mixture of 1 mM ammonium ferrous sulfate, 1mM sodium chloride, 50 mM sulfuric acid, and 500 mL triple distilled water was then slowly added to the agarose solution while constant stirring should be applied until the temperature was cooled to  $50^\circ\text{C}$ . To

## Report Documentation Page

<b>Report Date</b> 25 Oct 2001	<b>Report Type</b> N/A	<b>Dates Covered (from... to)</b> -
<b>Title and Subtitle</b> Measurement of Ferric Ion Diffusion Coefficient in Fricke-Infused Agarose Gel From MR Image Intensity Changes	<b>Contract Number</b>	
	<b>Grant Number</b>	
	<b>Program Element Number</b>	
<b>Author(s)</b>	<b>Project Number</b>	
	<b>Task Number</b>	
	<b>Work Unit Number</b>	
<b>Performing Organization Name(s) and Address(es)</b> Institutes of Biomedical Engineering and Radiological Sciences National Yang Ming University Pei-Tou Taipei, Taiwan, R.O.C.	<b>Performing Organization Report Number</b>	
<b>Sponsoring/Monitoring Agency Name(s) and Address(es)</b> US Army Research, Development & Standardization Group PSC 802 Box 15 FPO AE 09499-1500	<b>Sponsor/Monitor's Acronym(s)</b>	
	<b>Sponsor/Monitor's Report Number(s)</b>	
<b>Distribution/Availability Statement</b> Approved for public release, distribution unlimited		
<b>Supplementary Notes</b> Papers from 23rd Annual International Conference of the IEEE Engineering in Medicine and Biology Society, October 25-28, 2001, held in Istanbul, Turkey. See also ADM001351 for entire conference on cd-rom.		
<b>Abstract</b>		
<b>Subject Terms</b>		
<b>Report Classification</b> unclassified	<b>Classification of this page</b> unclassified	
<b>Classification of Abstract</b> unclassified	<b>Limitation of Abstract</b> UU	
<b>Number of Pages</b> 4		

compensate for the oxygen lost during the boiling process, the agarose solution was aerated during the cooling process. The agarose was then poured into cylindrical container in the skull phantom for gamma knife irradiation and MR imaging.

#### 5) MR imaging and dose mapping technique:

In our study, MR image is taken with the parameters: TR/TE: 500/11ms, slice thickness: 3mm, FOV: 26cm, matrix size: 256×256, and NEX: 2. A total of six images were taken. The first one is taken before Gamma Knife irradiated the gel phantom. The second is taken immediately after radiation. The rest four images were taken at a delay time of 13min, 32, 59, and 118 min after the second image.

Based on the Bloch equation and MR physics, it had been shown that for T1-weighted spin-echo image with  $TE \ll TR$ , the image intensity change ( $\Delta S$ ) is related to the absorbed dose ( $D_s$ ) [6],

$$\Delta S = k \times [1 - \exp(-TR(aD_s + b))] \quad (3)$$

where  $TR$  is the repetition time,  $TE$  is the echo time,  $k$ ,  $a$ ,  $b$  were the coefficients related to proton density, combined relaxation rates contributed from water, ferric ions and ferrous ions in gel which could be determined by non-linear regression.

#### 6) Least square ferric ion diffusion coefficient calculation:

From Eq. (2),  $\tilde{\rho}(\mathbf{k}, t)$  can be obtained from  $\tilde{\rho}(\mathbf{k}, 0)$  by multiplying it with  $\exp(-D|\mathbf{k}|^2 t)$ , where  $\tilde{\rho}(\mathbf{k}, 0)$  is the 3D-FFT of  $\rho(x, y, z, 0)$  and  $\tilde{\rho}(\mathbf{k}, t)$  is the 3D-FFT of  $\rho(x, y, z, t)$ . With the four different  $\tilde{\rho}(\mathbf{k}, t)$ ,  $t = 13\text{min}, 32\text{min}, 59\text{min}$  and  $118\text{min}$ , we can derive the expected intensity change  $\Delta S(\rho)$  using Eq. (3). Because diffusion follows the convolution process shown in Eq. (2), we can find out the actual diffusion coefficient,  $D$ , in a least square sense, by choosing the value that minimizes the standard error between expected values and experimental values for any arbitrary  $D$ .

### III. RESULTS

Fig 1 illustrated the image intensity change ( $\Delta S$ ) before and after irradiation.

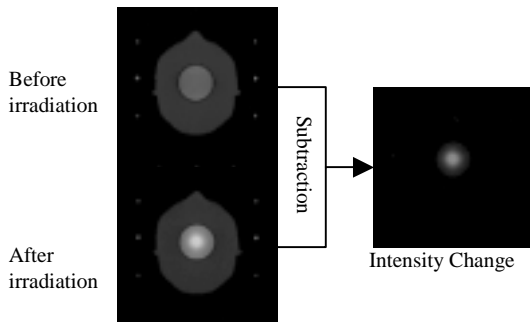


Fig. 1 Image intensity change due to irradiation.

Fig. 2 is the dose-response characteristic curve in our image-based MRI-Fricke-infused gel dosimetry.

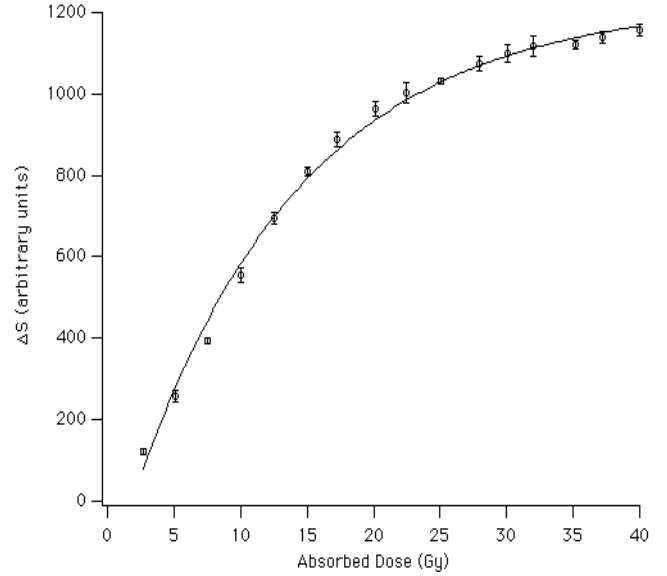


Fig. 2 Dose response curve of the Fricke-agarose dosimeter gel used in this study. Error bar stands for one standard deviation.

The mapping function based on Eq. (3) where  $k$ ,  $a$ , and  $b$  coefficients were determined by non-linear regression for the dose-response data.:

$$\Delta S = 1070.8 \{1 - \exp[-0.5(0.17D_s - 0.34)]\} \quad (4)$$

Effect of ferric ion diffusion for a designated elapsed time can be illustrated in Fig. 3. The difference of image intensity ( $\Delta S$ ) was derived by subtracting the reference image (image acquired before irradiation) from the image acquired after an elapsed diffusion time of 13 min, 32 min, 59 min, and 118 min. For better visual representation, the differences of the intensity values were scaled by five. Since difference of image intensity ( $\Delta S$ ) in the Eq. (4) is fitted by using the differences between the reference image and the image acquired immediately after the irradiation; i.e. no diffusion effect is considered, so that if we substitute the difference of image intensity in Fig. 3 into the inverse function of Eq. (4), the predicted dose value distribution will be affected by the ferric ion diffusion effect.

Fig. 4 (a) illustrated the initial dose distribution denoted by  $\rho(x, y, z, 0)$  which was generated by the point dose calculation algorithm. Although the maximum dose value located in focal point is 40 Gy, the image intensity had been scaled to the 8-bit gray level image (with maximum intensity of 255). Fig. 4 (b) is the corresponding difference of image intensity ( $\Delta S$ )

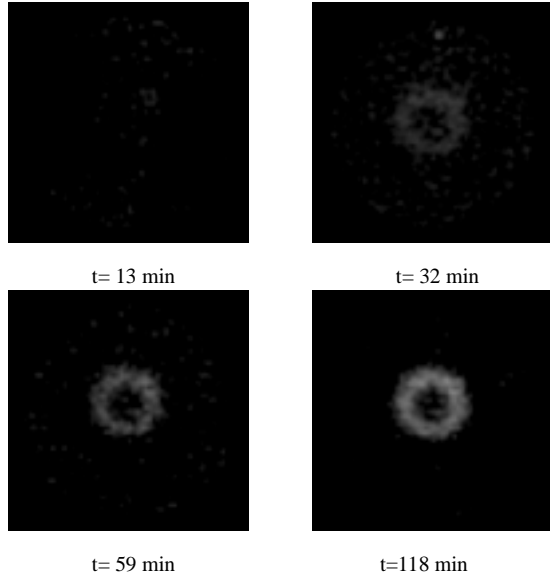


Fig 3. The diffusion effect in a time elapse MR images obtained with a delay diffusion time of 13 min, 32 min, 59 min, and 118 min.

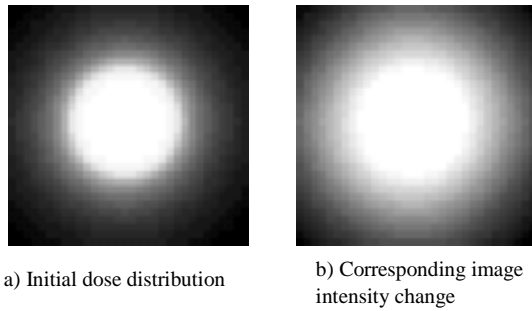
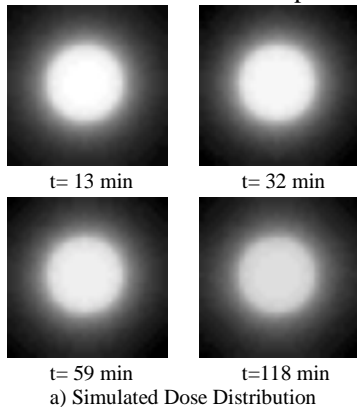
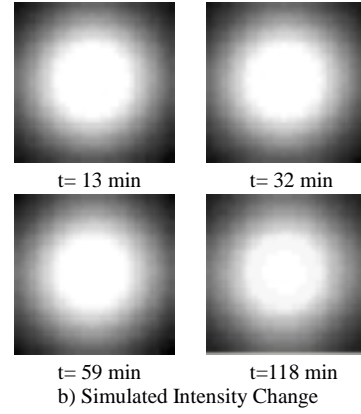


Fig 4 Initial dose distribution and its corresponding image intensity change generated by our simulation model.

Fig. 5 (a) (b) represented the new dose distribution and its corresponding image intensity change when diffusion effect is considered for a delayed time of 13 min, 32 min, 59 min, 118 min. They are generated by multiplying the diffusion factor  $\exp(-D|\mathbf{k}|^2t)$  with diffusion coefficient  $D$  equals to  $1.31 \times 10^{-2} \text{cm}^2\text{h}^{-1}$  to the 3D FFT of the original dose distribution according to Eq. (2) and then take the inverse 3D FFT for the corresponding time  $t$ .



a) Simulated Dose Distribution



b) Simulated Intensity Change

Fig 5. (a) (b) The simulated dose distribution diagrams and their corresponding image intensity changes.

Table 1 and Fig 6 display the normalized standard error for different diffusion coefficients between  $1.20 \times 10^{-2} \text{cm}^2\text{h}^{-1} \sim 1.49 \times 10^{-2} \text{cm}^2\text{h}^{-1}$  we applied in our simulation process. Obviously we can find that the local minimum emerged at  $D = 1.31 \times 10^{-2} \text{cm}^2\text{h}^{-1}$ .

TABLE I  
NORMALIZED STANDARD ERROR BETWEEN SIMULATION MATRIX AND  
EXPERIMENTAL RESULTS FOR DIFFERENT DIFFUSION COEFFICIENTS

Diffusion coefficient $D$ ( $\text{cm}^2\text{h}^{-1}$ )	Normalized Standard Error
$1.21 \times 10^{-2}$	18152.5453
$1.23 \times 10^{-2}$	18147.7398
$1.25 \times 10^{-2}$	18144.0284
$1.27 \times 10^{-2}$	18141.3925
$1.29 \times 10^{-2}$	18139.8138
$1.31 \times 10^{-2}$	18139.2743
$1.33 \times 10^{-2}$	18139.7566
$1.35 \times 10^{-2}$	18141.2435
$1.37 \times 10^{-2}$	18143.7180
$1.39 \times 10^{-2}$	18147.1636

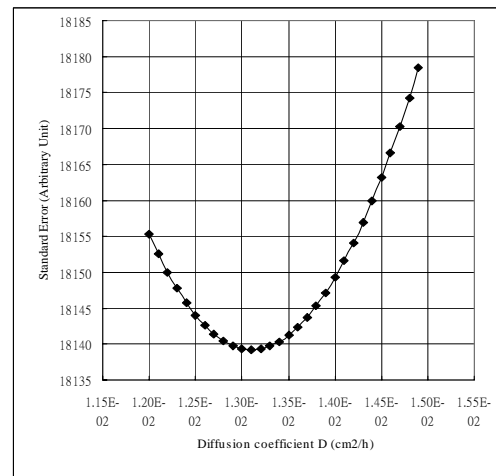


Fig. 6 Standard errors vs. diffusion coefficients.

#### IV. DISCUSSION

The obtained diffusion coefficient coincides within the  $1 \sim 2 \times 10^{-2} \text{cm}^2 \text{h}^{-1}$  range reported by previous studies under varying concentrations of gel ingredients.

The entire simulation process can be illustrated in the flowchart in Fig. 7.

Fig 4 (b) shows more bright regions than Fig. 4 (a) since Eq. 4 enhanced greater contrast in low dose region.

The displays of simulation results in Fig. 5 (a) and (b) were both expanded to a 16-bit gray level image (with maximum intensity of 255) which might not be similar to the experimental result in Fig. 3.

#### V. CONCLUSION

A simple approach involving fast image-based dosimetry technique to estimate the diffusion coefficient of ferric ions is proposed. With this information at hand, it is possible to consider calibrating the dose distribution deteriorations as a function of time and to deduced ways to alleviate this undesired ferric ion diffusion effects.

#### ACKNOWLEDGMENT

This work is supported by the National Science Council (Grant No: NSC 89-2320-B-010-078).

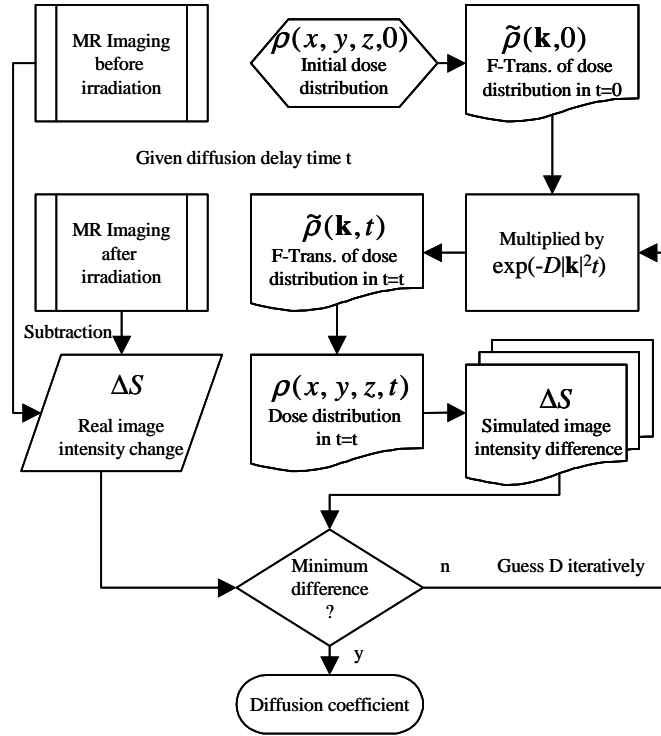


Fig. 7 The entire simulation flowchart.

#### REFERENCES

- [1] Gore JC, Kang YS, and Schulz RJ. Measurement of radiation dose distributions by nuclear magnetic resonance imaging. *Phys Med Biol* 1984;29:1189-1197.
- [2] Olsson LE, Arndt J, Fransson A, *et al.* Three-dimensional dose mapping from gamma knife treatment using a dosimeter gel and MR-imaging. *Radiotherapy Oncol* 1992;24:82-86.
- [3] Schulz RJ, deGuzman AF, Nguyen DB, *et al.* Dose-response curves for Fricke-infused agarose gels as obtained by nuclear magnetic resonance. *Phys Med Biol* 1990;35:1611-1622.
- [4] Olsson LE, Petersson S, Westrin BA, *et al.* Diffusion of ferric ions in agarose dosimeter gels. *Phys Med Biol* 1992;37:2243-2252.
- [5] Harris PJ, Piercy A, and Baldock C. A method for determining the diffusion coefficient in Fe(II/III) radiation dosimetry gels using finite elements. *Phys Med Biol* 1996;41:1745-1753 (1996).
- [6] Balcom BJ, Lee TJ, Sharp AR, *et al.* Diffusion in Fe(II/III) radiation dosimetry gels measured by magnetic resonance imaging. *Phys Med Biol* 1995;40:1665-1676.
- [7] Chu WC, Guo WY, Wu MC, *et al.* The radiation induced magnetic resonance image intensity change provides a more efficient three-dimensional dose measurement in MRI-Fricke-agarose gel dosimetry. *Med Phys* 1998;25:2326-2332.
- [8] Pedersen TV, Olsen DR, and Skretting A. Measurement of the ferric ion diffusion coefficient in agarose and gelatine gels by utilization of the evolution of a radiation induced edge as reflected in relaxation rated images. *Phys Med Biol* 1997;42:1575-1585.
- [9] Kron T, Jonas D, and Pope JM. Fast T<sub>1</sub> imaging of dual gel samples for diffusion measurements in nmr dosimetry gels. *Magn Reson Imaging* 1997;15:211-221
- [10] Chu WC, and Wang J. Exploring the concentration gradient dependency of ferric ion diffusion effect in MRI-Fricke-infused gel dosimetry. *Phys Med Biol* 2000;45:L63-L64..